Three-dimensional biomimetic vascular model reveals a RhoA, Rac1, and *N*-cadherin balance in mural cell–endothelial cell-regulated barrier function

Stella Alimperti[a,b,c,1], Teodelinda Mirabella[a,b,c,1], Varnica Bajaj[a,b], William Polacheck[a,b,c], Dana M. Pirone[d], Jeremy Duffield[e,f,g], Jeroen Eyckmans[a,b,c], Richard K. Assoian[h,i], and Christopher S. Chen[a,b,c,2]

[a]Department of Biomedical Engineering, Boston University, Boston, MA 02215; [b]Biological Design Center, Boston University, Boston, MA 02215; [c]The Wyss Institute for Biologically Inspired Engineering at Harvard, Harvard University, Boston, MA 02115; [d]Department of Science, Mount St. Mary's University, Emmitsburg, MD 21727; [e]Division of Nephrology, Department of Medicine, University of Washington, Seattle, WA 98195; [f]Department of Pathology, University of Washington, Seattle, WA 98195; [g]Institute of Stem Cell and Regenerative Medicine, University of Washington, Seattle, WA 98195; [h]Department of Systems Pharmacology and Translational Therapeutics, University of Pennsylvania, Philadelphia, PA 19104; and [i]Program in Translational Biomechanics, Institute of Translational Medicine and Therapeutics, University of Pennsylvania, Philadelphia, PA 19104

Edited by Shu Chien, University of California, San Diego, La Jolla, CA, and approved July 7, 2017 (received for review November 4, 2016)

The integrity of the endothelial barrier between circulating blood and tissue is important for blood vessel function and, ultimately, for organ homeostasis. Here, we developed a vessel-on-a-chip with perfused endothelialized channels lined with human bone marrow stromal cells, which adopt a mural cell-like phenotype that recapitulates barrier function of the vasculature. In this model, barrier function is compromised upon exposure to inflammatory factors such as LPS, thrombin, and TNFα, as has been observed in vivo. Interestingly, we observed a rapid physical withdrawal of mural cells from the endothelium that was accompanied by an inhibition of endogenous Rac1 activity and increase in RhoA activity in the mural cells themselves upon inflammation. Using a system to chemically induce activity in exogenously expressed Rac1 or RhoA within minutes of stimulation, we demonstrated RhoA activation induced loss of mural cell coverage on the endothelium and reduced endothelial barrier function, and this effect was abrogated when Rac1 was simultaneously activated. We further showed that *N*-cadherin expression in mural cells plays a key role in barrier function, as CRISPR-mediated knockout of *N*-cadherin in the mural cells led to loss of barrier function, and overexpression of *N*-cadherin in CHO cells promoted barrier function. In summary, this bicellular model demonstrates the continuous and rapid modulation of adhesive interactions between endothelial and mural cells and its impact on vascular barrier function and highlights an in vitro platform to study the biology of perivascular–endothelial interactions.

3D culture | mural cells | vascular inflammation | RhoGTPases | *N*-cadherin

Barrier properties of blood vessels play a major role in organ function and homeostasis (1). Upon tissue injury, activation of inflammatory cascades causes a loss of barrier function, which results in fluid leakage into the interstitial tissue, ultimately leading to edema. When blood and platelets are exposed to the underlying extracellular matrix, clotting and further inflammation can also be triggered. Thus, in acute settings, such as in ischemic or hemorrhagic stroke, massive changes in barrier function can compromise vital organs (2, 3). Even mild but prolonged loss of barrier function can ultimately result in compromised perfusion, chronic inflammation, and tissue damage (4–7).

Although endothelial cells (ECs) are the primary effectors of barrier control, it has long been appreciated that there is a supporting mesenchymal population known as mural cells that are important for modulating endothelial function. Vascular mural cells are a heterogeneous cell population consisting of vascular smooth muscle cells and pericytes, which were defined originally based on their anatomical location, covering the abluminal surface and sharing the basement membrane with the endothelium of capillaries, arterioles, and venules (8, 9). The functional role of mural cells is to modulate vessel function by regulating blood flow, blood vessel contractility, vascular integrity, and, overall, organ homeostasis (10–14). For example, for proper organ function in kidney and brain, where barrier properties in the microvasculature need to be finely tuned, an appropriate mural cell–EC ratio is important (15–17). Whereas mural cells are thought to be important in vivo, much of our understanding of barrier function regulation is focused solely on the endothelium (18, 19). This may be, in part, because barrier function is widely studied in endothelial monolayers (20, 21) and is also due to the lack of an in vitro system that incorporates both ECs and mural cells, which can be exposed to fluid flow (22).

Here, we have developed a biomimetic 3D platform that recapitulates perivascular-mediated barrier function in an engineered microvessel with a perfusable lumen and then investigated whether inflammatory cues would impact the endothelial–mural cell interaction. We showed that both primary human bone marrow stromal cells (hBMSCs) and pericytes reside perivascularly and adopt mural functions within the engineered vasculature. Interestingly, we found that vascular inflammation induces a Ras homolog family member A (RhoA)-dependent detachment of mural cells and reduces *N*-cadherin–mediated coverage of vessels, leading to vascular permeability. Furthermore, we were able to substantiate these

Significance

Organ homeostasis requires integrity of blood vessels; alterations or disruption of the vascular barrier between blood and tissue contribute to numerous diseases. Endothelial cells and mural cells are two key cell types, which play significant roles for the maintenance of barrier function. Here, we present a 3D bicellular vascular model to mimic this barrier function and study the role of mural cells in vascular inflammation. Importantly, by using this 3D model we identified RhoA, Rac1, and *N*-cadherin as important regulators in mural–endothelial cell-mediated vascular barrier function. Given the recognized fundamental importance of this barrier in numerous disease settings, this in vitro microphysiological system presented herein could provide a tool for studying vascular barrier function in 3D microenvironments.

Author contributions: S.A., T.M., R.K.A., and C.S.C. designed research; S.A., T.M., and V.B. performed research; W.P., D.M.P., and J.D. contributed new reagents/analytic tools; S.A. and T.M. analyzed data; and S.A., T.M., J.E., and C.S.C. wrote the paper.

The authors declare no conflict of interest.

This article is a PNAS Direct Submission.

Freely available online through the PNAS open access option.

[1]S.A. and T.M. contributed equally to this work.

[2]To whom correspondence should be addressed. Email: chencs@bu.edu.

This article contains supporting information online at www.pnas.org/lookup/suppl/doi:10.1073/pnas.1618333114/-/DCSupplemental.

findings in an in vivo model of LPS-driven skin inflammation. Hence, our 3D bicellular system enables us to deconvolute the contribution of different blood vessel cell types on vascular barrier function and to detect molecular targets for potential therapeutics to treat blood vessel diseases.

Results

Bicellular Perfusable 3D Platform Recapitulates Pericyte Role in Regulating Vascular Barrier Function. To study the role of perivascular cells in regulating barrier function, we used a microfluidic device in which human bone marrow stromal cells (hBMSCs), a cell population that exhibit mural cell characteristics (23–28), lined a perfusable endothelialized channel. The device was assembled based largely on previously described models of endothelialized channels (29), in this case by casting a single, hollowed cylindrical channel (160 μm diameter) into type-I collagen within a polydimethylsiloxane (PDMS) mold containing a bulk chamber hosting the vessel and reservoir chambers for introducing media into the system. hBMSCs were seeded 4 h before ECs and allowed to adhere and spread on the collagen wall (Fig. 1*A*). After hBMSCs were allowed to adhere to the collagen (~4 h), human umbilical vein endothelial cells (HUVECs) were seeded into the vessel mold. Within 24 h, the cells organized into an engineered microvessel within our device and consisted of an inner layer of endothelial cells connecting to each other through platelet endothelial cell adhesion molecule (PECAM-1 or CD31, Fig. 1*B*), VE-cadherin, and JAM-A (*SI Appendix*, Fig. S1) surrounded by an outer layer of hBMSCs. Akin to anatomical organization of pericytes in vivo, the hBMSCs decorated the abluminal surface of the confluent endothelium in our device (Fig. 1*B*) along the longitudinal axis of the microvessel and expressed the mural membrane surface markers PDGFRβ, NG2, desmin, CD146, and RSG5 (30–33) (*SI Appendix*, Fig. S2). To evaluate whether our vascular chip recapitulates in vivo barrier-like features of vessels and whether hBMSCs contribute to that barrier, we seeded different ratios of hBMSCs to HUVECs (0:1, 1:1, 1:5, 1:10, and 1:100) (*SI Appendix*, Fig. S3) and quantified permeability by measuring the extravasation of fluorescently labeled 10 kDa or 70 kDa dextran from the vessel lumen (34) (Fig. 1*C*). We found that the presence of hBMSCs in ratios of 1:1 and 1:5 relative to HUVECs significantly reduced leakage of fluorescent dextran into the interstitial space compared with control microvessels containing ECs alone. Further decreasing the ratio of hBMSCs-HUVECs (from 1:1 to 1:100) resulted in dye extravasation, indicating increased vascular permeability (Fig. 1*C*). To further validate that hBMSCs are indeed an appropriate cell type to study barrier function, we compared the vascular permeability of endothelialized channels covered with human kidney pericytes (PCs), hBMSCs, and human lung fibroblasts (hFs). Whereas hFs reduced permeability compared with HUVECs alone, the effect was much smaller than the near complete reduction in permeability seen with either hBMSCs or PCs (*SI Appendix*, Fig. S4). In contrast to hFs, hBMSCs do not exhibit migratory behavior, and they cover the endothelium by sharing the basement membrane with ECs (*SI Appendix*, Fig. S5 *A* and *B*), thus further reinforcing that hBMSCs emulate vascular mural cells anatomically and functionally in our model. Taken together, our findings demonstrate that a coculture model comprised of an endothelialized channel covered with hBMSCs is a valid model for studying EC–mural cell interactions in the context of barrier function.

Inflammatory Factors Impair Mural Coverage and Permeability. To examine mural cell behavior during inflammation, we introduced different proinflammatory stimuli into the chip, including lipopolysaccharides (*LPS*) (100 ng/mL), thrombin (THBN) (0.3 U/mL), and tumor necrosis factor alpha (TNFα) (50 ng/mL), each of which has been shown to affect vascular integrity and endothelial blood barrier function (20, 21, 35–37), although the contribution of mural cells in this response is unclear. One hour after treatment in bicellular microvessels, we measured an increase in permeability of 20-fold (LPS), 25-fold (THBN), and twofold (TNFα), compared with the untreated (CTRL) bicellular microvessels (Fig. 2*A*). Interestingly, we observed that treatment with these proinflammatory

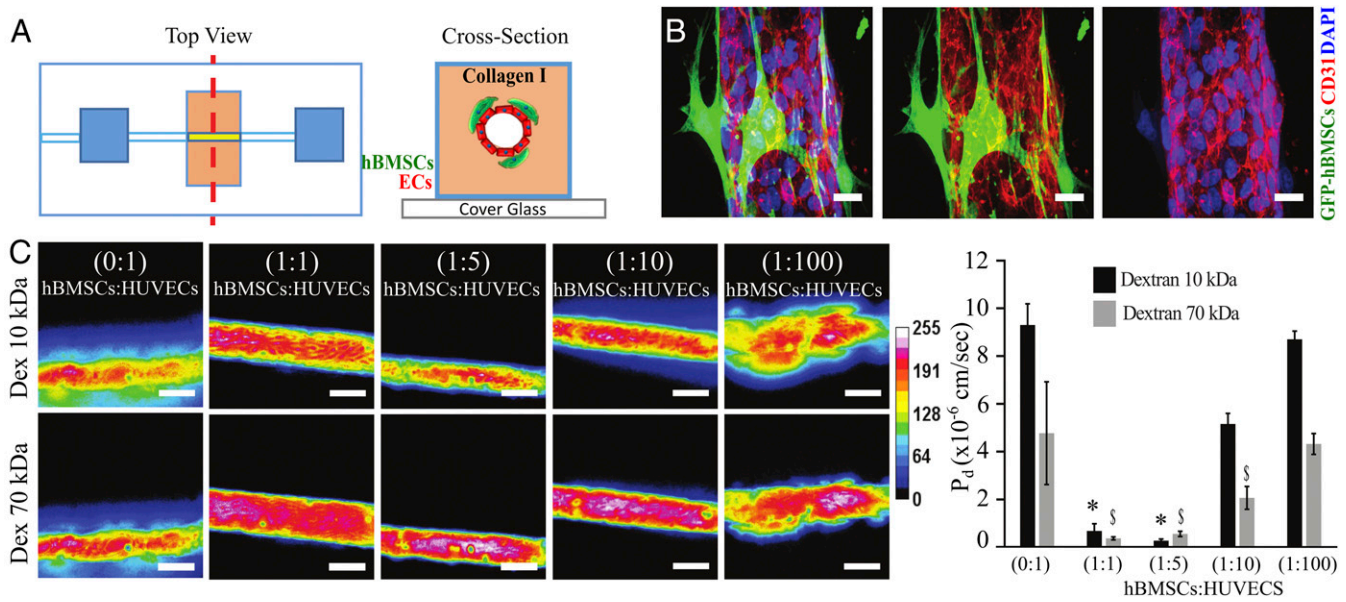

Fig. 1. Three-dimensional biomimetic platform to study mural–endothelial cell interaction and vascular barrier function. (*A*) Device schematic mimicking mural cell-mediated barrier function. A cylindrical channel is formed in a 3D collagen matrix within a microfabricated PDMS gasket. GFP-hBMSCs cells and the endothelial cells (ECs), HUVECs, were seeded in the device. (*B*) Representative confocal immunofluorescence images showing the formed endothelial vessel surrounded by GFP-hBMSCs; HUVECs were stained for CD31 (red), and GFP-hBMSCs cells were stained for anti-GFP antibody (green) and nuclei for DAPI (blue). (Scale bar, 20 μm.) (*C*) Heat map panels are relative to dextran diffusion of different molecular sizes (10 and 70 kDa) traced 2 min after dye injection into device, measured across devices seeded with different ratios of GFP–hBMSCs:HUVECs. (Scale bar, 100 μm.) Histogram reports diffusive permeability coefficient (P_d) in different ratios of hBMSCs:ECs. Data are expressed as mean ± SEM. $N = 6$. *, P value < 0.05; $, P value < 0.05.

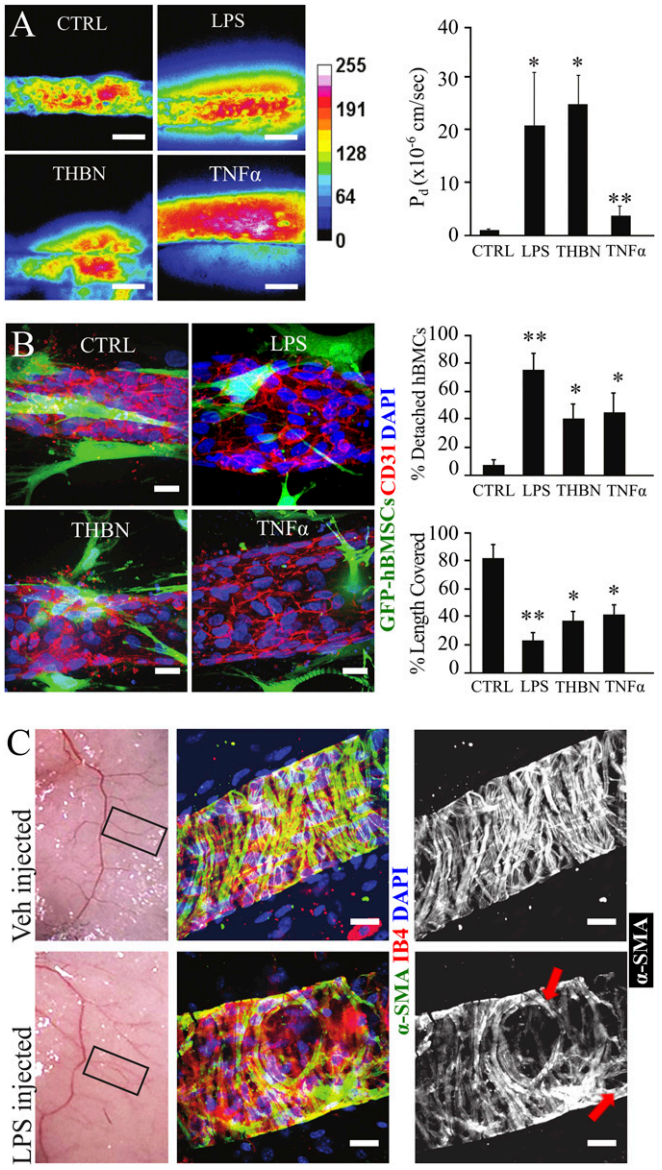

Fig. 2. Modeling vascular inflammation on a chip. (*A*) Representative heat map panel of 70 kDa Texas Red dextran perfused into the engineered microvessels treated with LPS (100 ng/mL), Thrombin (THBN) (0.3 U/mL), or TNFα (10 ng/mL) and compared with untreated (CTRL) vessels. Histogram reports the diffusive permeability coefficient (P_d) for the different treatments. (Scale bar, 100 μm.) Data are expressed as mean ± SEM. $N = 6$. *, P value < 0.05; **, P value < 0.01. (*B*) Representative images of engineered microvessels not treated (CTRL) or treated with LPS, THBN, or TNFα; HUVECs were stained for CD31 (red), and GFP-hBMSCs cells were stained using an anti-GFP antibody (green) and counterstained with DAPI (blue). (Scale bar, 20 μm.) Histograms reported detached hBMSCs (percent of total hBMSCs per field of view) and vascular length covered by hBMSCs (percent of total length) in the different treatment groups. Data are expressed as mean ± SEM. $N = 9$ (three fields of view per device, three devices). *, P value < 0.05; **, P value < 0.01. (*C*) Gross appearance of skin injected with Vehicle (Veh) or LPS. Skin vessels were immunostained for IB4 (red) labeling endothelium and α-SMA (green) labeling vascular mural cells (perivascular cells), and nuclei are counterstained with DAPI (blue), revealing openings (red arrows) within the mural wall of inflamed skin vasculature. (Scale bar, 20 μm.)

cytokines caused the hBMSCs to either detach or cover a smaller portion of endothelium (Fig. 2*B*). Specifically, after LPS treatment, ~70–80% of hBMSCs assumed a migratory phenotype, with protrusions extending further into the interstitial matrix, and the few cells left in contact with the endothelium only covered 20% of the vascular length. Almost half of hBMSCs were detached when treated with THBN and TNFα, and the remaining adherent cells covered only 40% of the vascular length (Fig. 2*B*). We further confirmed our in vitro findings in an in vivo model of s.c. LPS-mediated inflammation. Thirty minutes after LPS injection, abdominal skin was dissected, whole-mount stained for endothelial [isolectin B4 (IB4)] and smooth muscle cell marker (α-SMA), and vessels (50 to 100 μm in diameter) branching from the abdominal epigastric bundle were imaged. Similar to in vitro observations, acute inflammation, as induced by LPS, caused openings in the perivascular part of those vessels, and the vascular surface covered by α-SMA positive cells was visibly reduced compared with vessels of untreated (Veh) skin (Fig. 2*C*). Taken together, these data demonstrate that inflammatory cytokines induced detachment of mural cells from vessels and showed a concomitant increase in vascular permeability.

Inflammatory Cues Drive Mural Cell Detachment and Vascular Permeability via Changes in Pericyte Rho GTPase Signaling. It has been shown that several proinflammatory cytokines induce junction disruption directly in ECs in part through activation of RhoA signaling (20, 21, 37–39). We asked whether RhoA would be activated in hBMSCs upon inflammatory stimuli. Indeed, we found an increase in active GTP-loaded RhoA levels and a decrease in GTP-loaded Ras-related C3 botulinum toxin substrate 1 (Rac1) in hBMSCs treated with LPS, THBN, and TNFα (Fig. 3*A*). To investigate the role of this increased RhoA activity in vascular mural cells and function, we first blocked Rho-associated coiled-coil–containing protein kinase (ROCK), a major downstream effector of RhoA, with the inhibitor Y27632 (10 μM) and asked whether this might rescue barrier function in our system. Indeed, Y27632 abrogated the hyperpermeability induced by LPS treatment,

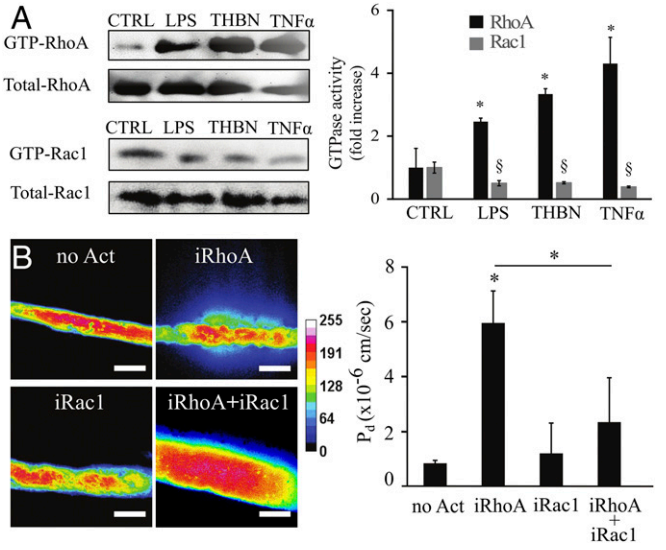

Fig. 3. Modulation of RhoGTPase activity in mural cells under inflammatory conditions. (*A*) Active GTP-RhoA and GTP-Rac1 were assessed by pull-down assay after treatment with LPS (100 ng/mL), Thrombin (THBN) (0.3 U/mL), or TNFα (10 ng/mL) and compared with an untreated control (CTRL). Amounts of GTP-RhoA and GTP-Rac were normalized to the total RhoA or Rac1, respectively. Data are expressed as mean ± SEM. $N = 3$. *, P value < 0.05; §, P value < 0.05. (*B*) Representative heat map panel of 70 kDa Texas Red dextran perfused into the engineered microvessels under no activation (no Act), RhoA activation (iRhoA;12.5 μM GA_3-AM), Rac1 activation (iRac1;25 nM Rapalog), and RhoA+Rac1 activation (iRhoA+iRac1;12.5 μM GA_3-AM + 25 nM Rapalog). (Scale bar, 100 μm.) Histogram reports the diffusive permeability coefficient (P_d) for the considered different activation. Data are expressed as mean ± SEM. At least $N = 6$. *, P value < 0.05.

restoring barrier function (*SI Appendix*, Fig. S6), but it was unclear whether the effect was due to inhibition of ROCK in the mural cells or in the endothelium. We therefore turned to a genetic approach to directly target RhoA activity in mural cells. hBMSCs were transduced with lentivirus harboring (*i*) a RhoA(CA) activating mutant, but lacking its endogenous farnesylation site, thus preventing membrane localization and activation; and (*ii*) a membrane-tethered anchor, in which the addition of gibberellin-analog (GA_3-AM) induced coupling of the RhoA construct to the membrane-tethered anchor to rapidly activate the construct (40). hBMSCs expressing these constructs but not yet exposed to gibberellin behaved normally, adhered to the endothelialized channel similar to nontransduced cells, and maintained confluency and barrier function of endothelium (Fig. 3*B*). When GA_3-AM (12.5 μM, for 1 h) was given to induce RhoA activity (iRhoA) in hBMSCs within the engineered vessels, the permeability of the vessel to fluorescently labeled 70 kDa dextran was significantly up-regulated (Fig. 3*B*). Interestingly, the RhoA-activated hBMSCs were less spread, highly detached from the endothelium (70% of total hBMSCs), and covered only 20% of endothelial length (*SI Appendix*, Fig. S7), phenocopying what we observed upon treatment with proinflammatory cytokines. Similar to RhoA-activated hBMSCs, activation of RhoA in endothelium triggered hBMSC detachment from the endothelium, indicating that RhoA signaling in both cell types regulates mural cell behavior (*SI Appendix*, Fig. S8*A*).

Given that Rac1 can be anticorrelated with RhoA signaling (41) we asked whether overexpression of Rac1 modulates RhoA-induced vascular permeability. To address this question, we transfected RhoA-expressing hBMSCs with a Rac1 construct featuring another orthogonal chemical dimerization system to gibberellin-analog, Rapalog, that induced Rac1 localization to the plasma membrane to enable activation. Indeed, exposure to Rapalog (25 nM, for 1 h) (iRac1) rescued vascular barrier function (Fig. 3*B*). Taken together, these findings suggest that inflammation up-regulates RhoA activity and down-regulates Rac1 activity in hBMSCs, resulting in a reduction of vessel coverage by the hBMSCs, and these changes increase vascular leakage.

Inflammation Disrupts hBMSCs–Endothelial Junctional *N*-cadherin to Impact Barrier Function. Given that inflammatory factors reduced the mural cell coverage of the endothelium, we hypothesized that under inflammatory conditions, heterotypic cell–cell adhesion is impaired between endothelial and mural cells. The main adhesion molecule responsible for mediating interactions between the two cell types is *N*-cadherin (42, 43). Using antibody staining, we found *N*-cadherin to be abundantly located at the interface between ECs and hBMSCs in normal conditions (Fig. 4*A*). In contrast, the signal for *N*-cadherin appeared more diffuse in cocultures treated with LPS or in RhoA (iRhoA) activated hBMSCs (Fig. 4*A*). Similarly, RhoA (iRhoA) activated HUVECs showed disrupted junctions with their neighboring ECs or hBMSCs (*SI Appendix*, Fig. S8*B*), thus confirming the role of small GTPases in junction stability (44). To directly examine whether *N*-cadherin engagement might contribute to barrier function, we treated our engineered vessels with neutralizing antibodies against the extracellular domain of *N*-cadherin (N-cad Ab) and observed a massive increase in permeability compared with the microvessels treated with IgG isotype control (IgG) (Fig. 4*B*). However, *N*-cadherin junctions exist homotypically between neighboring ECs, and thus the antibody approach could not isolate the contribution of mural cells to the response. To specifically investigate the role of *N*-cadherin in hBMSCs, we blocked *N*-cadherin expression in hBMSCs using a CRISPR-mediated approach (*SI Appendix*, Fig. S9*A*). Indeed, the permeability increased significantly in microvessels composed of *N*-cadherin–deleted hBMSCs (Fig. 4*C*). To test whether the role of *N*-cadherin in mediating barrier function is conserved in other perivascular cells as well, we knocked out *N*-cadherin in human primary smooth muscle cells (SMCs) and human kidney pericytes (PCs) and showed that permeability increased when *N*-cadherin is deleted in these cell populations (*SI Appendix*, Fig. S10). Finally, to investigate whether *N*-cadherin is sufficient to support barrier function, we overexpressed *N*-cadherin in CHO cells to see if they could phenocopy the effects of mural cells on endothelial barrier function (*SI Appendix*, Fig. S9*B*). Indeed, endothelialized channels lined abluminally with *N*-cadherin–expressing CHO cells displayed lower permeability than endothelialized channels with control CHO cells (Fig. 4*D*). Together, these findings indicate that junctional *N*-cadherin between mural and endothelial cells is a key mediator of barrier function.

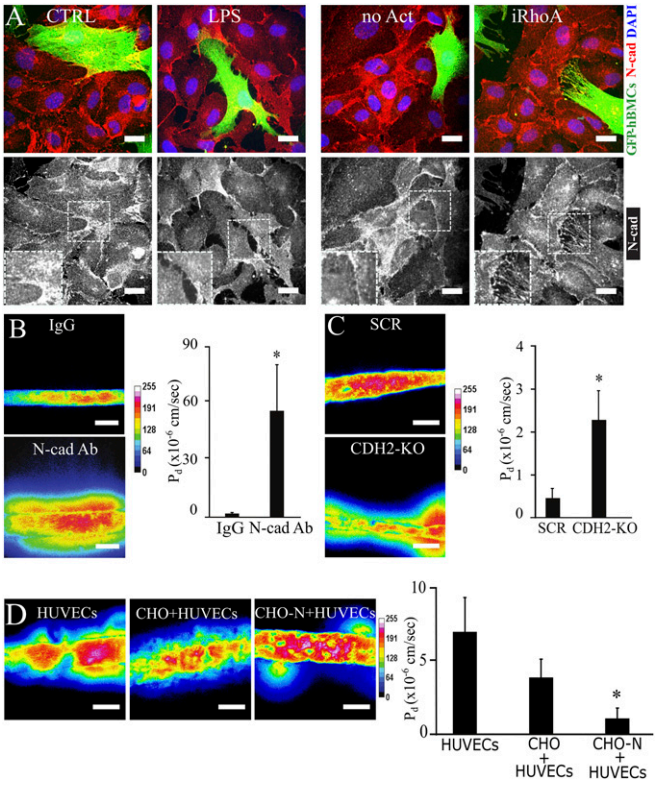

Fig. 4. *N*-cadherin (*N*-cad)–mediated permeability in inflammation and in RhoA-activated mural cells. (*A*) Representative confocal immunofluorescence images *N*-cadherin (red) in monolayers of HUVECs covered with GFP–hBMSCs (green, anti-GFP antibody staining) under no treatment (CTRL) or LPS treatment and no activation (no Act) or RhoA activation (iRhoA). Nuclei are counterstained with DAPI (blue). (Scale bar, 20 μm.) (*B*) Representative heat map panel of 70 kDa Texas Red dextran perfused into the engineered microvessels treated with IgG isotype (IgG) or *N*-cadherin–blocking antibody (N-cad Ab). (Scale bar, 100 μm.) Histogram reports the diffusive permeability coefficient (P_d) for the different treatments. (*C*) Representative heat map panel of 70 kDa Texas Red dextran perfused into the engineered microvessels holding scrambled (SCR) and CDH2 knockout (CDH2-KO) hBMSCs. (Scale bar, 100 μm.) Histogram reports the diffusive permeability coefficient (P_d) under scrambled and CDH2 knockout conditions. (*D*) Representative heat map panel of 70 kDa Texas Red dextran perfused into the engineered microvessels holding HUVECs, HUVECs+CHO, and HUVECs+CHO-N (CHO cells overexpressing *N*-cadherin). (Scale bar, 100 μm.) Histogram reports the diffusive permeability coefficient (P_d) under HUVECs, HUVECs+CHO, and HUVECs+CHO-N conditions. Data are expressed as mean ± SEM. $N = 6$. *, P value < 0.05.

Discussion

Perivascular cells have been implicated in diseases related to chronic inflammation and fibrosis, especially in organs such as kidney, liver, and skin (45, 46). Activated mural cells, pericytes in particular, have been shown to detach from local capillaries and migrate to sites of chronic injury (47–49), where they can be major contributors to the

myofibroblast population such as during skin, muscle, renal, and lung fibrosis (50–55). Here, we provide a demonstration in a culture setting that mural cells detach from the endothelium and migrate away from the vessel, and this can occur rapidly during acute exposure to proinflammatory cytokines. The ability to recapitulate this migratory effect in culture, where the concentrations of cytokines are highest at the vessels (versus the interstitial spaces), suggests an active process whereby cytokine stimulation drives mural cells into the matrix and not via a chemoattractant mechanism, as has previously been postulated (56). Given that mural cells dynamically alter their adhesions with the endothelium, this suggests a more active role for mural–endothelial interactions in acute responses than perhaps was previously appreciated.

Several groups have reported that inflammatory stimuli, such as thrombin and LPS, activate the RhoA pathway in endothelium, leading to disruption of cell–cell contact and thus directly increasing vascular permeability (36, 44, 57). RhoA activation is known to disrupt cell–cell adhesions (involving cadherins) by increasing the tension on the cadherin bonds (58–62), but primarily in a context where Rac1 is also down-regulated (63). Here in our study we find that RhoA is activated in mural cells in response to inflammatory stimuli. By using methods to rapidly activate RhoA either at the membrane of mural cells or in endothelial cells, we demonstrate that hyperactive RhoA disrupts EC-PC adhesion, and this cell–cell adhesion is important for the ability of PCs to reinforce barrier function. Concomitant with RhoA activation, we observed a suppression of Rac1 signaling and showed that activating Rac1 in the PCs stabilizes junctional integrity and barrier function even when RhoA is activated. These findings are consistent with previous studies, demonstrating a role for Rac1 in stabilizing junctions (64–66), and more generally opposing roles for Rac1 and RhoA in driving numerous cell functions (41, 67–70). Further understanding the underlying mechanisms by which Rac1 and RhoA impact PC signaling, structural organization, and function will lead to a deeper appreciation for how these cells contribute to vascular function.

N-cadherin is a critical adhesion receptor that mediates cell–cell coupling in neuronal or mesenchymal populations. Among perivascular cells such as hBMSC-derived mural cells or SMCs, *N*-cadherin not only supports homotypic cell–cell adhesion, but also regulates proliferation and differentiation (71, 72). Although ECs primarily mediate barrier function through tight junctions and VE-cadherin–mediated adherens junctions, they also express *N*-cadherin and are thus able to form heterotypic cell interactions with other populations, for example, with smooth muscle cells, cardiomyocytes. EC-specific loss of *N*-cadherin causes embryonic lethality (73, 74), and thus, whereas *N*-cadherin has been implicated as a receptor that could mediate heterotypic cell–cell interactions, it has been difficult to demonstrate the contribution of cell-type–specific *N*-cadherin to the interaction. In addition to *N*-cadherin demonstrated here, other cell–cell junctions, including gap junctional proteins, connexin-43 (CX43), may also be involved in mural–endothelial regulation (8, 75). In our study, gain and loss-of-function of *N*-cadherin indicate that *N*-cadherin engagement between mural cells and ECs is essential for retaining vascular barrier function and illustrates how cell-based biomimetic platforms can be used to isolate contributions of different cell types and molecular players in complex tissue functions.

A deeper understanding of human pathophysiology requires the development of robust on-chip systems that can recapitulate the structures, mechanics, and complex cell–cell interactions that occur in vivo (76–80). Whereas we demonstrate herein the feasibility to capture these interactions in on-chip systems, a challenge in the future is to establish tissue-specific features of vascular beds such as low permeable brain vasculature (blood brain barrier) or high permeable liver sinusoids consisting of endothelial cells with fenestrae. Our culture platform captures the essential features of a simplified vasculature, consisting of a perfused vessel lined with a polarized endothelium surrounded by mural cells, and an interstitial extracellular matrix context for perivascular cells to freely remodel between cell–cell and cell–matrix interactions. As a result, these features provide a platform for better understanding the contributions of endothelial cells, mural cells, and their interactions in pathophysiological contexts such as inflammation and thus offers a powerful complement to animal models for understanding this important physiologic structure.

Materials and Methods

To determine the permeability of endothelial monolayers and endothelial–mural cocultures in vitro, microvessels were formed in microfluidic devices as described previously (29). Cells were seeded in 160-μm diameter tubes formed in collagen type I hydrogels to create lumenized microvessels. Ten and seventy kilodaltons of dextran was perfused through the vessel lumens, and extravasation of the dextrans was measured as a function of time to quantify the diffusive permeability (34). Human kidney pericytes (PCs) were purified from fetal human kidneys. Informed permission for the use of fetal tissues was obtained from all patients. The isolation of cells was approved by the University of Washington Institutional Review Board (IRB447773EA) and performed at the University of Washington Medical Center as previously described (81). Details of the materials and methods for this study can be found in *SI Appendix, SI Materials & Methods*.

Statistical analysis of the data was performed using ANOVA one-way test. *P* value was set to be significant if <0.05, unless differently stated in the text.

ACKNOWLEDGMENTS. We thank Thomas Ferrante for his help in Leica SP5 X MP Inverted Confocal Microscope (SP5XMP) and for image analysis. This work was supported in part by grants from the National Institutes of Health (EB08396, UH3EB017103, HL115553) and the Biological Design Center at Boston University. V.B. acknowledges support from Undergraduate Research Scholars Award (UROP), and W.P. acknowledges support from NIH training Grant Ruth L. Kirschstein National Research Service Award (HL129733).

1. Weiss N, Miller F, Cazaubon S, Couraud PO (2009) The blood-brain barrier in brain homeostasis and neurological diseases. *Biochim Biophys Acta* 1788:842–857.
2. Hall CN, et al. (2014) Capillary pericytes regulate cerebral blood flow in health and disease. *Nature* 508:55–60.
3. Yemisci M, et al. (2009) Pericyte contraction induced by oxidative-nitrative stress impairs capillary reflow despite successful opening of an occluded cerebral artery. *Nat Med* 15:1031–1037.
4. Claesson-Welsh L (2015) Vascular permeability–the essentials. *Ups J Med Sci* 120: 135–143.
5. Sutton TA (2009) Alteration of microvascular permeability in acute kidney injury. *Microvasc Res* 77:4–7.
6. Garcia JG (2009) Concepts in microvascular endothelial barrier regulation in health and disease. *Microvasc Res* 77:1–3.
7. Duffield JS (2014) Cellular and molecular mechanisms in kidney fibrosis. *J Clin Invest* 124:2299–2306.
8. Winkler EA, Bell RD, Zlokovic BV (2011) Central nervous system pericytes in health and disease. *Nat Neurosci* 14:1398–1405.
9. Stratman AN, Schwindt AE, Malotte KM, Davis GE (2010) Endothelial-derived PDGF-BB and HB-EGF coordinately regulate pericyte recruitment during vasculogenic tube assembly and stabilization. *Blood* 116:4720–4730.
10. Rucker HK, Wynder HJ, Thomas WE (2000) Cellular mechanisms of CNS pericytes. *Brain Res Bull* 51:363–369.
11. Hirschi KK, D'Amore PA (1996) Pericytes in the microvasculature. *Cardiovasc Res* 32: 687–698.
12. Bergers G, Song S (2005) The role of pericytes in blood-vessel formation and maintenance. *Neuro-oncol* 7:452–464.
13. Das A, et al. (1988) ATP causes retinal pericytes to contract in vitro. *Exp Eye Res* 46: 349–362.
14. Stratman AN, Davis GE (2012) Endothelial cell-pericyte interactions stimulate basement membrane matrix assembly: influence on vascular tube remodeling, maturation, and stabilization. *Microsc Microanal* 18:68–80.
15. Bell RD, et al. (2010) Pericytes control key neurovascular functions and neuronal phenotype in the adult brain and during brain aging. *Neuron* 68:409–427.
16. Winkler EA, Sengillo JD, Bell RD, Wang J, Zlokovic BV (2012) Blood-spinal cord barrier pericyte reductions contribute to increased capillary permeability. *J Cereb Blood Flow Metab* 32:1841–1852.
17. Kramann R, Humphreys BD (2014) Kidney pericytes: Roles in regeneration and fibrosis. *Semin Nephrol* 34:374–383.
18. Sukriti S, Tauseef M, Yazbeck P, Mehta D (2014) Mechanisms regulating endothelial permeability. *Pulm Circ* 4:535–551.

19. Mehta D, Malik AB (2006) Signaling mechanisms regulating endothelial permeability. *Physiol Rev* 86:279–367.
20. Dejana E, Simionescu M, Wolburg H (2009) Endothelial cell biology and pathology. *Cell Tissue Res* 335:1–3.
21. Dejana E, Tournier-Lasserve E, Weinstein BM (2009) The control of vascular integrity by endothelial cell junctions: Molecular basis and pathological implications. *Dev Cell* 16:209–221.
22. He Y, Yao Y, Tsirka SE, Cao Y (2014) Cell-culture models of the blood-brain barrier. *Stroke* 45:2514–2526.
23. Gaengel K, Genové G, Armulik A, Betsholtz C (2009) Endothelial-mural cell signaling in vascular development and angiogenesis. *Arterioscler Thromb Vasc Biol* 29:630–638.
24. Au P, Tam J, Fukumura D, Jain RK (2008) Bone marrow-derived mesenchymal stem cells facilitate engineering of long-lasting functional vasculature. *Blood* 111:4551–4558.
25. da Silva Meirelles L, Bellagamba BC, Camassola M, Nardi NB (2016) Mesenchymal stem cells and their relationship to pericytes. *Front Biosci (Landmark Ed)* 21:130–156.
26. Tian X, Brookes O, Battaglia G (2017) Pericytes from Mesenchymal Stem Cells as a model for the blood-brain barrier. *Sci Rep* 7:39676.
27. Bautch VL (2011) Stem cells and the vasculature. *Nat Med* 17:1437–1443.
28. Crisan M, Corselli M, Chen WC, Péault B (2012) Perivascular cells for regenerative medicine. *J Cell Mol Med* 16:2851–2860.
29. Nguyen DH, et al. (2013) Biomimetic model to reconstitute angiogenic sprouting morphogenesis in vitro. *Proc Natl Acad Sci USA* 110:6712–6717.
30. Armulik A, Genové G, Betsholtz C (2011) Pericytes: Developmental, physiological, and pathological perspectives, problems, and promises. *Dev Cell* 21:193–215.
31. Winkler EA, Bell RD, Zlokovic BV (2010) Pericyte-specific expression of PDGF beta receptor in mouse models with normal and deficient PDGF beta receptor signaling. *Mol Neurodegener* 5:32.
32. Lindahl P, et al. (1998) Paracrine PDGF-B/PDGF-Rbeta signaling controls mesangial cell development in kidney glomeruli. *Development* 125:3313–3322.
33. Bianco P, et al. (2013) The meaning, the sense and the significance: translating the science of mesenchymal stem cells into medicine. *Nat Med* 19:35–42.
34. Adamson RH, Lenz JF, Curry FE (1994) Quantitative laser scanning confocal microscopy on single capillaries: Permeability measurement. *Microcirculation* 1:251–265.
35. Giannotta M, Trani M, Dejana E (2013) VE-cadherin and endothelial adherens junctions: Active guardians of vascular integrity. *Dev Cell* 26:441–454.
36. Wallez Y, Huber P (2008) Endothelial adherens and tight junctions in vascular homeostasis, inflammation and angiogenesis. *Biochim Biophys Acta* 1778:794–809.
37. Dejana E, Orsenigo F, Molendini C, Baluk P, McDonald DM (2009) Organization and signaling of endothelial cell-to-cell junctions in various regions of the blood and lymphatic vascular trees. *Cell Tissue Res* 335:17–25.
38. Spindler V, Schlegel N, Waschke J (2010) Role of GTPases in control of microvascular permeability. *Cardiovasc Res* 87:243–253.
39. Dejana E, Orsenigo F, Lampugnani MG (2008) The role of adherens junctions and VE-cadherin in the control of vascular permeability. *J Cell Sci* 121:2115–2122.
40. Miyamoto T, et al. (2012) Rapid and orthogonal logic gating with a gibberellin-induced dimerization system. *Nat Chem Biol* 8:465–470.
41. Burridge K, Doughman R (2006) Front and back by Rho and Rac. *Nat Cell Biol* 8: 781–782.
42. Paik JH, et al. (2004) Sphingosine 1-phosphate receptor regulation of N-cadherin mediates vascular stabilization. *Genes Dev* 18:2392–2403.
43. Armulik A, Abramsson A, Betsholtz C (2005) Endothelial/pericyte interactions. *Circ Res* 97:512–523.
44. Yao L, et al. (2010) The role of RhoA/Rho kinase pathway in endothelial dysfunction. *J Cardiovasc Dis Res* 1:165–170.
45. Greenhalgh SN, Iredale JP, Henderson NC (2013) Origins of fibrosis: Pericytes take centre stage. *F1000Prime Rep* 5:37.
46. Pober JS, Sessa WC (2014) Inflammation and the blood microvascular system. *Cold Spring Harb Perspect Biol* 7:a016345.
47. Göritz C, et al. (2011) A pericyte origin of spinal cord scar tissue. *Science* 333:238–242.
48. Lin SL, et al. (2011) Targeting endothelium-pericyte cross talk by inhibiting VEGF receptor signaling attenuates kidney microvascular rarefaction and fibrosis. *Am J Pathol* 178:911–923.
49. Ren S, et al. (2013) LRP-6 is a coreceptor for multiple fibrogenic signaling pathways in pericytes and myofibroblasts that are inhibited by DKK-1. *Proc Natl Acad Sci USA* 110: 1440–1445.
50. Dulauroy S, Di Carlo SE, Langa F, Eberl G, Peduto L (2012) Lineage tracing and genetic ablation of ADAM12(+) perivascular cells identify a major source of profibrotic cells during acute tissue injury. *Nat Med* 18:1262–1270.
51. Faulkner JL, Szcykalski LM, Springer F, Barnes JL (2005) Origin of interstitial fibroblasts in an accelerated model of angiotensin II-induced renal fibrosis. *Am J Pathol* 167:1193–1205.
52. Lin SL, Kisseleva T, Brenner DA, Duffield JS (2008) Pericytes and perivascular fibroblasts are the primary source of collagen-producing cells in obstructive fibrosis of the kidney. *Am J Pathol* 173:1617–1627.
53. Humphreys BD, et al. (2010) Fate tracing reveals the pericyte and not epithelial origin of myofibroblasts in kidney fibrosis. *Am J Pathol* 176:85–97.
54. Rock JR, et al. (2011) Multiple stromal populations contribute to pulmonary fibrosis without evidence for epithelial to mesenchymal transition. *Proc Natl Acad Sci USA* 108:E1475–E1483.
55. Kisseleva T, et al. (2012) Myofibroblasts revert to an inactive phenotype during regression of liver fibrosis. *Proc Natl Acad Sci USA* 109:9448–9453.
56. Schrimpf C, Teebken OE, Wilhelmi M, Duffield JS (2014) The role of pericyte detachment in vascular rarefaction. *J Vasc Res* 51:247–258.
57. Loirand G, Guérin P, Pacaud P (2006) Rho kinases in cardiovascular physiology and pathophysiology. *Circ Res* 98:322–334.
58. Daneshjou N, et al. (2015) Rac1 functions as a reversible tension modulator to stabilize VE-cadherin trans-interaction. *J Cell Biol* 208:23–32.
59. de Rooij J, Kerstens A, Danuser G, Schwartz MA, Waterman-Storer CM (2005) Integrin-dependent actomyosin contraction regulates epithelial cell scattering. *J Cell Biol* 171:153–164.
60. Huynh J, et al. (2011) Age-related intimal stiffening enhances endothelial permeability and leukocyte transmigration. *Sci Transl Med* 3:112ra122.
61. Reinhart-King CA, Fujiwara K, Berk BC (2008) Physiologic stress-mediated signaling in the endothelium. *Methods Enzymol* 443:25–44.
62. Kohn JC, Lampi MC, Reinhart-King CA (2015) Age-related vascular stiffening: Causes and consequences. *Front Genet* 6:112.
63. Liu Z, et al. (2010) Mechanical tugging force regulates the size of cell-cell junctions. *Proc Natl Acad Sci USA* 107:9944–9949.
64. Waschke J, et al. (2004) Requirement of Rac activity for maintenance of capillary endothelial barrier properties. *Am J Physiol Heart Circ Physiol* 286:H394–H401.
65. Baumer Y, Spindler V, Werthmann RC, Bünemann M, Waschke J (2009) Role of Rac 1 and cAMP in endothelial barrier stabilization and thrombin-induced barrier breakdown. *J Cell Physiol* 220:716–726.
66. Wójciak-Stothard B, Potempa S, Eichholtz T, Ridley AJ (2001) Rho and Rac but not Cdc42 regulate endothelial cell permeability. *J Cell Sci* 114:1343–1355.
67. Chauhan BK, Lou M, Zheng Y, Lang RA (2011) Balanced Rac1 and RhoA activities regulate cell shape and drive invagination morphogenesis in epithelia. *Proc Natl Acad Sci USA* 108:18289–18294.
68. Bustos RI, Forget MA, Settleman JE, Hansen SH (2008) Coordination of Rho and Rac GTPase function via p190B RhoGAP. *Curr Biol* 18:1606–1611.
69. Ohta Y, Hartwig JH, Stossel TP (2006) FilGAP, a Rho- and ROCK-regulated GAP for Rac binds filamin A to control actin remodelling. *Nat Cell Biol* 8:803–814.
70. Jou TS, Nelson WJ (1998) Effects of regulated expression of mutant RhoA and Rac1 small GTPases on the development of epithelial (MDCK) cell polarity. *J Cell Biol* 142:85–100.
71. Mui KL, et al. (2015) N-cadherin induction by ECM stiffness and FAK overrides the spreading requirement for proliferation of vascular smooth muscle cells. *Cell Rep* 10: 1477–1486.
72. Alimperti S, You H, George T, Agarwal SK, Andreadis ST (2014) Cadherin-11 regulates both mesenchymal stem cell differentiation into smooth muscle cells and the development of contractile function in vivo. *J Cell Sci* 127:2627–2638.
73. Luo Y, Radice GL (2005) N-cadherin acts upstream of VE-cadherin in controlling vascular morphogenesis. *J Cell Biol* 169:29–34.
74. Liebner S, Cavallaro U, Dejana E (2006) The multiple languages of endothelial cell-to-cell communication. *Arterioscler Thromb Vasc Biol* 26:1431–1438.
75. Hirschi KK, Burt JM, Hirschi KD, Dai C (2003) Gap junction communication mediates transforming growth factor-beta activation and endothelial-induced mural cell differentiation. *Circ Res* 93:429–437.
76. Herland A, et al. (2016) Distinct Contributions of Astrocytes and Pericytes to Neuroinflammation Identified in a 3D Human Blood-Brain Barrier on a Chip. *PLoS One* 11: e0150360.
77. van der Helm MW, van der Meer AD, Eijkel JC, van den Berg A, Segerink LI (2016) Microfluidic organ-on-chip technology for blood-brain barrier research. *Tissue Barriers* 4:e1142493.
78. Benam KH, et al. (2016) Small airway-on-a-chip enables analysis of human lung inflammation and drug responses in vitro. *Nat Methods* 13:151–157.
79. Kim HJ, Li H, Collins JJ, Ingber DE (2016) Contributions of microbiome and mechanical deformation to intestinal bacterial overgrowth and inflammation in a human gut-on-a-chip. *Proc Natl Acad Sci USA* 113:E7–E15.
80. Alonzo LF, Moya ML, Shirure VS, George SC (2015) Microfluidic device to control interstitial flow-mediated homotypic and heterotypic cellular communication. *Lab Chip* 15:3521–3529.
81. Leaf IA, et al. (2017) Pericyte MyD88 and IRAK4 control inflammatory and fibrotic responses to tissue injury. *J Clin Invest* 127:321–334.